One-Pot Synthesis of Hollow Au_3Cu_1 Spherical-like and Biomineral Botallackite $Cu_2(OH)_3Cl$ Flowerlike Architectures Exhibiting Antimicrobial Activity

Min-Tien Hsiao,[†] Shin-Fu Chen,[†] Dar-Bin Shieh,*[,‡] and Chen-Sheng Yeh*[,†]

Department of Chemistry and Center for Micro/Nano Technology Research Department of Dentistry and Institute of Oral Medicine, National Cheng Kung University, Tainan 701, Taiwan

Received: August 26, 2005; In Final Form: November 5, 2005

A new form of Au_3Cu_1 hollow nanostructure was prepared by the reaction of Cu nanoparticles with $HAuCl_4$. Following a course of aging, the biomineral botallackite $Cu_2(OH)_3Cl$ nanoflowers were developed with the aid of Au_3Cu_1 hollow nanostructures at room temperature. It was proposed that the hollow nanospheres could serve as active centers for heterogeneous nucleation and mediated a mineralization process. Scanning electron microscopy and high-resolution transmission electron microscopy indicated that the nanoflowers are three-dimensional in appearance with a range of 500 nm − to 1 μm in size and made of several nanopetals with about 25 nm in thickness. In addition, we found that the shape separation could be achieved by using cationic cetyltrimethylammonium bromide to filter the different morphology spherical- and flowerlike structures due to the negative charge of hollow nanospheres. Both hollow nanospheres and nanoflowers presented antimicrobial activity toward *Streptococcus aureus* with MIC_{50} at 39.6 and 127.2 μg/mL, respectively.

Introduction

Biominerals growing in organisms have a variety of functions in biology. Biomineralization of inorganic minerals involves the delicate manipulation and refinement of properties. Thus, bioinorganic solids have inspired extensive studies in biology, chemistry, crystal engineering, and material science for the purpose of developing and refining new materials. As compared with the biominerals made of Ca-, Ba-, Fe-, and Si-based minerals, Cu-based biominerals are rather less common in living organisms. Recently, the first copper-containing mineral atacamite, $Cu_2(OH)_3Cl$, was discovered in the teeth of the carnivorous marine worm *Glycera*.[1] The atacamite $Cu_2(OH)_3Cl$ exhibits unusual mechanical properties of hardness and stiffness. $Cu_2(OH)_3Cl$ occurs in four polymorphic phases, atacamite, botallackite, clinoatacamite, and paratacamite. With regard to the synthesis of nanoscale materials, there was only one study performed by Chen et al. to prepare atacamite $Cu_2(OH)_3Cl$ nanoribbons.[2] Herein, we present the first example of three-dimensional botallackite $Cu_2(OH)_3Cl$ nanoflower architectures via hollow nanospheres-mediated process at room temperature.

Fabrication of complex architectures with three-dimensional or highly ordered nanostructures is highly desirable in current materials synthesis, holding the promise of advanced applications in electronics and optoelectronics. For example, 3D flowerlike MoS_2 nanostructures were manipulated by a thermal evaporation process, and they exhibited good capability in field emission due to the existence of the open edges in their nanopetals.[3] The current methods for the manipulation of 3D intricate flowerlike nanostructures are by high-temperature physical/chemical vapor deposition[3−6] and chemical solution routes including hydrothermal,[7,8] solvothermal,[9] and the slow solution-based metal salt reduction (usually requiring a reaction period of at least a day).[10−12] In this paper, we demonstrated a mild mineralization which was proposed through a hollow nanospheres-mediated process. The mineralization was performed at room temperature in aerobic circumstances, and the growth of $Cu_2(OH)_3Cl$ nanoflowers could be seen after a reaction period as short as 90 min. First, a new form of Au_3Cu_1 hollow nanosphere was prepared from the system of $Cu_{(nanoparticles)}-HAuCl_4$. In preparation, Cu nanoparticles were obtained by laser ablation of CuO powder in 2-propanol. Subsequently, the resulting Cu colloidal solution was mixed with $HAuCl_4$. The consequence of the reaction (less than 1 min) resulted in the formation of Au_3Cu_1 porous nanocages. Upon increasing aging time, nanocages could serve as heterogeneous nucleation sites to activate a mineralization process for the growth of a 3D flowerlike nanostructure. Hollow nanostructures have many applications, such as catalysis, drug delivery, and chemical storage. The results shown here indicated the highly active property of the hollow nanospheres and demonstrated a new approach in material synthesis.

Many animals or plants synthesize materials with antimicrobial activity to protect them from biological attacks in their living environment.[13,14] The nanoflowers consisted of $Cu_2(OH)_3Cl$, which was recently discovered and presented in the teeth of carnivorous marine worm *Glycera*. It is intriguing to know whether these flowers in nanometer scale exhibit antimicrobial activity. We thus performed micro-MIC assays for both hollow nanospheres and the derived nanoflowers. For the antimicrobial activity assay, a serial 2-fold dilution of the nanoparticle solutions was performed and then incubated with 5×10^4 cfu of *Staphylococcus aureus* in a 96-well microtiter plate. Both MIC_{50} and MIC_{90} were defined as the minimal concentrations of the nanoparticles to achieve 50% and 90% growth inhibition of the bacteria, respectively, as referenced to the nontreatment control.

* To whom correspondence should be addressed. E-mail: csyeh@mail.ncku.edu.tw (C.-S.Y.); dshieh@mail.ncku.edu.tw (D.-B.S.).

[†] Department of Chemistry and Center for Micro/Nano Technology Research.

[‡] Department of Dentistry and Institute of Oral Medicine.

10.1021/jp054827x CCC: $33.50
Published on Web 12/08/2005

Experimental Section

Cu nanoparticles were generated by laser irradiation of CuO powder in 2-propanol.[15] Pyrex vials were used as containers to prepare the colloidal solutions. An unfocused Nd:YAG laser (Quantel Brilliant) operated at 10 Hz (5 ns pulse width) with a wavelength of 1064 nm was conducted through the opening into the vials containing 0.015 g of CuO powder and 5 mL of 2-propanol. The Cu colloidal solutions were prepared as follows: a laser intensity of 100 mJ/pulse was employed to irradiate the mixture including CuO powder and 2-propanol for 5 min, followed by centrifugation to remove the remaining CuO powder. Subsequently, the prepared solutions were illuminated for an additional 5 min. The resulting Cu colloidal solutions had a deep wine-red color. The ablated solutions were routinely stirred every 1 min in the course of irradiation.

In a typical preparation of hollow nanospheres and nanoflowers, 1.1 mL of as-synthesized Cu colloidal solution was added to 3×10^{-7} mol of $HAuCl_4$ (dehydrated) to form hollow nanospheres. After addition of $HAuCl_4$, the colloidal color changed immediately (<1 min) from wine-red to grayish blue. After setting this blue solution aside for 3 h, a precipitate of $Cu_2(OH)_3Cl$ was observed. All manipulations were carried out under aerobic conditions.

The antimicrobial activities of the hollow nanospheres and the nanoflowers were analyzed by micro-MIC broth dilution assay using a common human pathogen, the *Staphylococcus aureus* ATCC 29213 as a standard model. For the micro-MIC assay, the nanoparticles were first weighed and dissolved in 10μL of 2-propanol followed by addition of Trypticase soy broth (TSB; BBL Microbiology Systems, Cockeysville, MD) to a final concentration of 300 μg/mL. The nanoparticles containing TSB solutions were then transferred to a 96 well microtiter plate, and a serial 2-fold dilution to the final range of 300 μg/mL to 300 ng/mL at 100 μL/well was performed. The test standard bacteria were grown to the mid-log phase before being applied for the assay, which was determined by the growth curve analysis via spectroscopic absorption at 600 nm and the colony formation on TSB agar plate after serial dilution. The bacteria were diluted to a final concentration of 10^6 cfu/mL, and 100 μL of the solution was dispensed into each well that already contained 100 μL of test culture medium of different nanoparticle concentrations. Thus the initial final bacteria concentration in each well was 5×10^4 cfu, and the nanoparticle concentrations were in the range of 150 μg/mL to 150 ng/mL in a total of 200 μL of culture mixture per well. TSB containing the respective test concentrations of the nanoparticles served as the blank control, while bacteria growing in TSB alone without nanoparticles served as the no-treatment control for the analysis. The nanoparticles were co-incubated with the bacteria for 18 h at 37 °C under agitation. As a control, the bacteria were also cultured on plates to check their purity. After 12 h of incubation, the 96-well microtiter plates were scanned with an ELISA reader for the absorption at 600 nm wavelength. The MIC_{50} and the MIC_{90} were determined as the minimum nanoparticle concentrations to achieve 50 and 90% bacteria growth inhibition, respectively, as compared to the no-treatment control.

Results and Discussion

It is known that laser ablation can readily generate spherical nanoparticles (Figure 1). However, the particles formed in this way usually suffer from inhomogeneous particle sizes.[15] In this study, the resulting Cu nanoparticles had an average diameter of 44.9 ± 19.8 nm in size.

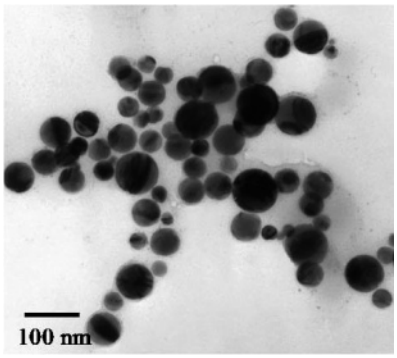

Figure 1. TEM image of the resulting Cu nanoparticles by laser irradiation of CuO powder in 2-propanol.

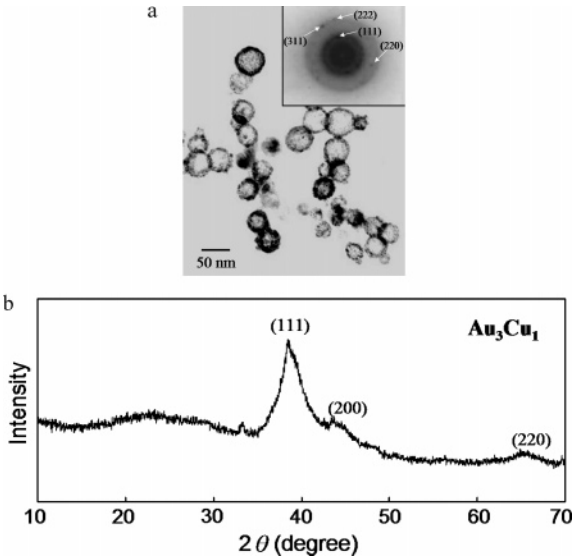

Figure 2. (a) TEM image of the porous Au_3Cu_1 nanospheres with hollow interiors produced by reaction of Cu nanoparticles with 3×10^{-7} mol of $HAuCl_4$ after 5 min. The inset shows the SAED of a single hollow nanosphere. (b) XRD pattern of the prepared Au_3Cu_1 hollow nanospheres by reaction of Cu nanoparticles with 3×10^{-7} mol of $HAuCl_4$ for 5 min.

Once the Cu nanoparticles were synthesized in 2-propanol, $HAuCl_4$ was added to Cu colloidal solution at room temperature. Figure 2a shows the transmission electron microscopy (TEM) image of the porous hollow nanospheres produced by reaction of Cu nanoparticles with 3×10^{-7} mol of $HAuCl_4$. The particle peripheries appear darker than their central portions, and the nanoshells are made of discrete particle domains, indicating the formation of the porous morphology. Apart from the preparation condition using a refluxing process by Xia et al.,[16] this hollow nanostructure process was completed at room temperature under aerobic conditions. The resulting nanocages have slightly larger average diameter of 48.9 ± 19.1 nm than those of Cu precursory particles. The porous nanoshells were measured as 5.8 ± 1.8 nm. Energy-dispersive X-ray (EDX) analysis was performed to assess the particle composition and showed the elements of both Au and Cu (see Supporting Information). The inset of Figure 2a displays the selected-area electron diffraction (SAED) pattern of an as-synthesized single hollow structure. Although the diffraction exhibited diffusion, indicating low crystallinity, all the rings could be indexed to Au_3Cu_1 composition. X-ray diffraction (XRD) measurements also revealed Au_3Cu_1 diffraction peaks with the broad band (Figure 2b).

Through mechanisms suggested by Xia et al.,[16] at the beginning of a galvanic replacement reaction in this system,

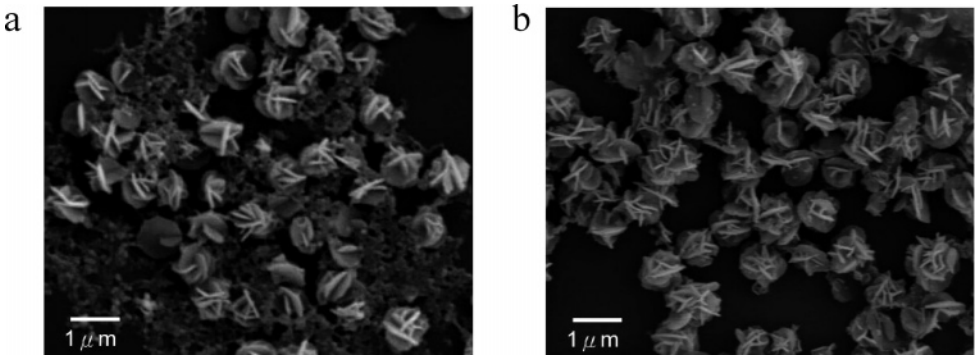

Figure 3. SEM images of resulting products after reaction of Cu nanoparticles with $HAuCl_4$ for 3 h (a) before CTAB separation and (b) after CTAB separation.

the deposition of Au atoms formed an incomplete layer on individual Cu nanoparticles. Subsequently, a hollow nanoshell was a reaction consequence of Cu nanoparticles with $HAuCl_4$ along with an alloying process. The standard reduction potential of $AuCl_4^-$/Au pair (0.99V vs SHE) is higher than those of Cu^{2+}/Cu (0.34V vs SHE) and Cu^+/Cu pairs (0.189V vs SHE) in aqueous solution. Although the reduction potentials might be varied in 2-propanol, it was likely to process the replacement reaction by etching of the Cu templates from $AuCl_4^-$ as well. The resulting Cu colloids have a characteristic surface plasmon absorption at 574 nm.[15] We have followed the UV−vis spectroscopic method to monitor the reaction between $HAuCl_4$ and Cu nanoparticles. As mentioned in the early, the colloidal color changed from wine-red to grayish blue in less than 1 min. The UV−vis behavior developed immediately from a sharp Cu plasmon band to a broad absorption near 650 nm (see Supporting Information).

Formation of the nanoparticle with a hollow interior could also be driven by the Kirkendall effect,[17] nicely demonstrated by Alivisatos et al. for spherical colloids at the nanometer scale.[18] A physical phenomenon relies on the differential diffusion rate of two species in a diffusion couple to create the voids inside the cores of the particles. Because Cu atoms diffuse faster than Au atoms,[19] the outward flow of Cu atoms into the Au−Cu alloying shell, resulting from the Au deposited on Cu colloid through a galvanic replacement reaction, leads to an evacuation of the core. We have found that the fabricated hollow nanospheres have a cavity size of only ∼83% of the Cu precursory particles in diameter, which might indicate the occurrence of inward Au through a Au−Cu shell as well. The shrinkage of the voids was also observed in the hollow spheres made of PbS by following the Kirkendall effect.[20] On the basis of size variation, the Kirkendall effect is proposed as likely to dominate direct solid evacuation in the case of Au_3Cu_1. Regarding the galvanic replacement reaction, the fabricated void size is mainly determined by the dimension of the nanoscale template precursor.[16] However, the materials usually form hollow crystals at an elevated temperature, as compared with room temperature introduced here, through the Kirkendall effect. At present, we cannot definitely clarify the driving force for the formation of nanospheres with hollow interiors.

As mentioned earlier, the reaction of forming hollow nanospheres occurred quickly (less than 1 min) by observing colloidal solution turning from wine-red to grayish blue after the addition of $HAuCl_4$. When the reaction solution was left still at room temperature for 3 h, a precipitate of Cu-based biomineral (copper hydroxide chloride) was formed. Figure 3a shows the SEM image of the resulting precipitates containing flowerlike architectures accompanying spherical-like hollow nanoparticles. Herein, we have introduced surfactant-assisted shape separation for the isolation of flower-shaped particles from a mixture of spheres and 3D flower-shaped structures. The ξ-potential measurements indicated that the as-synthesized hollow nanoparticles exhibited a negative surface charge of −18 mV. A cationic surfactant (cetyltrimethylammonium bromide, CTAB) was treated as a flotation reagent to separate hollow nanospheres and nanoflowers. In the separation process, 1 mL of CTAB (0.1 M) was added into 1 mL of reaction mixture followed by a series of centrifugation and washing procedures. Due to the cationic CTAB coating on the hollow nanospheres, these spherical nanocages could be dispersed in a 2-propanol medium and remained in supernatant after centrifugation. Most of the spherical particles could be removed from flowerlike particles by repeating the above shape separation procedures. These recovered hollow particles by CTAB were found, identified by UV−vis absorption and electron diffraction, to retain Au_3Cu_1 structure after following the growth of the nanoflowers. Figure 3b displays the SEM image of the resulting products with the aid of CTAB. Although there were still some residual spherical particles observed, a simple surfactant-assisted approach provided an efficient separation to obtain nanoflowers.

Figure 4a shows a scanning electron microscopy (SEM) image of an individual flowerlike feature at higher magnification. Typically, the as-synthesized nanoflower is three-dimensional in appearance with a range of 500 nm to 1 μm in size and made of several nanopetals. These ultrathin nanopetals are about 25 nm in thickness. The TEM image of a single nanoflower (Figure 4b) shows that the produced crystallites are thin nanostructured flakes, which are consistent with the morphological form observed by SEM. Figure 4c shows the SAED pattern corresponding to the nanoflower of Figure 4b. The inset of Figure 4c displays the SAED pattern of a single petal. All of these diffraction rings could be indexed to monoclinic $Cu_2(OH)_3Cl$ (botallackite). The HRTEM image in Figure 4d provides the structural detail, where the fringe spacing of ∼0.57 nm corresponds to the distance between two (100) lattice planes. The crystal structure of botallackite has been shown to form a $Cu_2(OH)_3Cl$ octahedral edge-sharing sheet parallel to {100}.[21] One copper atom occupies the octahedral site coordinated by five hydroxyls and one chlorine, whereas the other copper is octahedrally surrounded by four hydroxyls and two chlorines. In addition to SAED measurements, XRD and EDS were also performed to give the botallackite structure and elemental analysis (see Supporting Information).

We followed the growth process by conducting the time-dependent evolution of $Cu_2(OH)_3Cl$ nanoflower morphology using TEM and found that the crystal growth of $Cu_2(OH)_3Cl$ could take less than 90 min to complete 3D flowerlike assemblies (see Supporting Information). The nanopetal assembly of the resultant nanoflowers remains unclear. From the

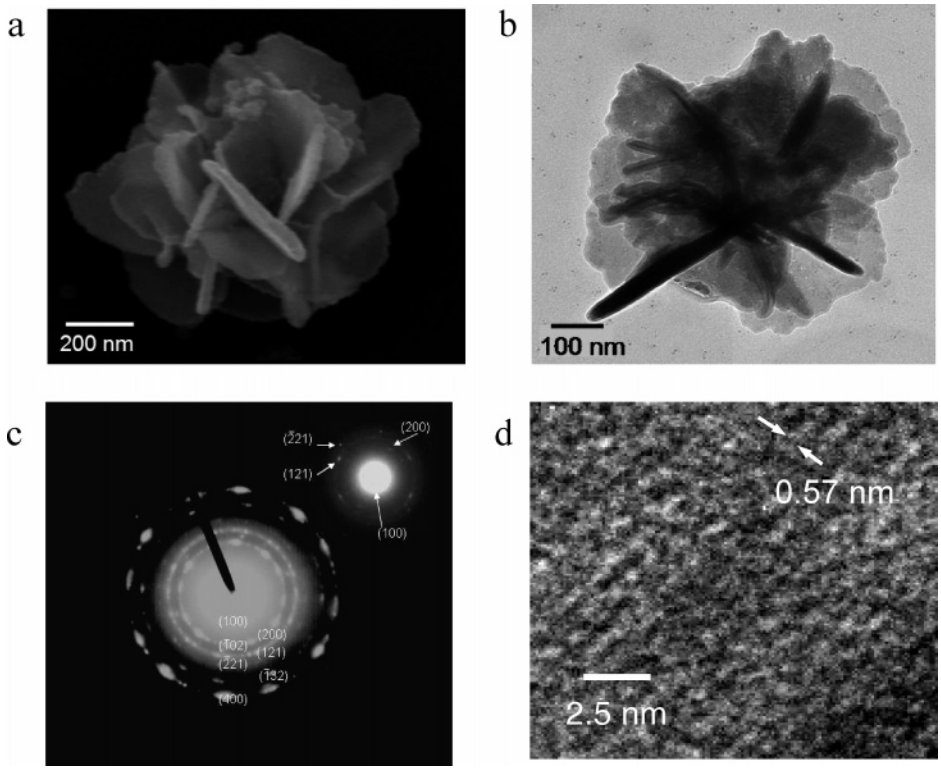

Figure 4. (a) A SEM image of a single nanoflower. (b) TEM image of a single nanoflower. (c) Selected area electron diffraction corresponding to Figure 3b and the inset showing the SAED from a single petal. (d) HRTEM image of a single petal showing the spacing of the lattice planes.

SCHEME 1

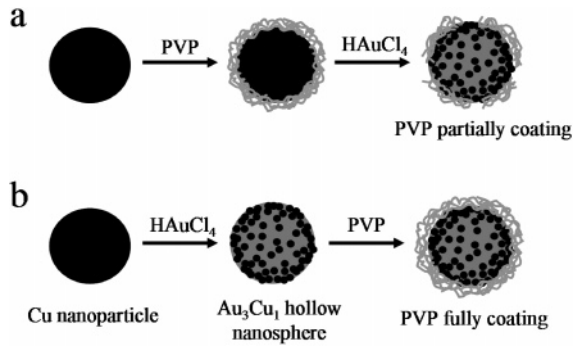

observed growth process, the nanopetals seem to grow on hollow nanospheres, which could serve as active centers for heterogeneous nucleation. The resulting hollow nanospheres are porous structures consisting of discrete particle domains. Thus, those domains formed on the shells provide numerous active sites and present a great deal of heterogeneous nucleation.

Accordingly, two parallel experiments were performed to further characterize the role of hollow nanospheres in the formation of $Cu_2(OH)_3Cl$ nanoflowers. These two experiments were designed to prepare hollow nanospheres with polyvinylpyrrolidone (PVP; MW, 40 000) polymer protection, but differed in the time of the addition of PVP, which resulted in different extents of protection on the hollow nanospheres, as shown in Scheme 1.[22]

Figure 5a shows the SEM image of the obtained product (case a) after 180 min of reaction. Some of the flakes revealed the similar morphology as the nanopetals of the nanoflowers shown in Figure 4a, but most of them showed the irregular shapes with no 3D nanoflower formation. The particles partially covered with PVP, where the flakes grew, were still Au_3Cu_1 nanospheres, and the flakes remained as $Cu_2(OH)_3Cl$. Although the porous particles with hollow interior were generated under this circumstance, the failure to produce nanoflowers is attributed to the existence of PVP laying on the outer surface of the hollow nanoparticles. Since Cu@PVP nanoparticles were synthesized first, the addition of $HAuCl_4$, which could have partly ruptured the PVP layer, resulted in porous nanocages and left some active sites of porous shell exposed. Thus, the incomplete heterogeneous nucleation caused the formation of flakelike structures only. For case b, the addition of PVP was performed after preparation of hollow nanospheres. Different from the partial coverage of PVP on the nanocage surface in case a, neither flowerlike nor flakelike features (Figure 5b) but spherical particles were observed from these hollow nanospheres fully coated with PVP. From the XRD measurements, these nanospheres with PVP fully covered shown in Figure 5b exhibited Au_3Cu_1 structure. On the basis of these results, the hollow nanospheres with porous structures were proposed to serve as a heterogeneous nucleation promoter and mediated the formation of 3D nanoflowers. Herein, we do not exclude the fact of the presence of PVP, which might influence the crystallization of $Cu_2(OH)_3Cl$.

Considering the reaction mechanisms, $Cu_2(OH)_3Cl$ could be ascribed to the following reaction scheme.

$$3Cu(s) + 2AuCl_4^- \rightarrow 2Au(s) + 3Cu^{2+} + 8Cl^- \quad (1)$$

$$H_2O \leftrightarrow H^+ + OH^- \quad (2)$$

$$2Cu^{2+} + Cl^- + 3OH^- \rightarrow Cu_2(OH)_3Cl \quad (3)$$

where H_2O likely originates from the moisture of the air. Throughout the experiments, formation of $Cu_2(OH)_3Cl$ nanoflowers was performed in aerobic conditions. Therefore, a controlled experiment was conducted in an Ar atmosphere, and only spherical particles were seen in the absence of flowerlike product (see Supporting Information). In addition, an experiment

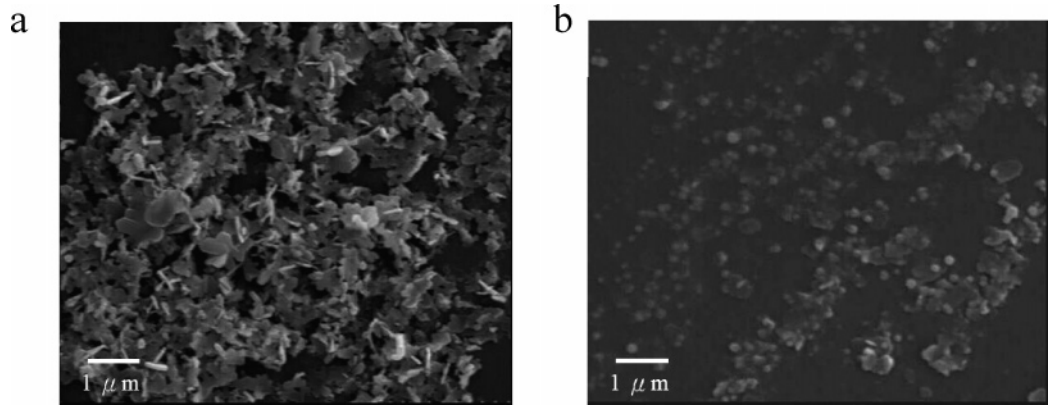

Figure 5. SEM images of the obtained products (a) indicating mainly irregular flakes from case a in Scheme 1 and (b) showing spherical particle observed from case b in Scheme 1.

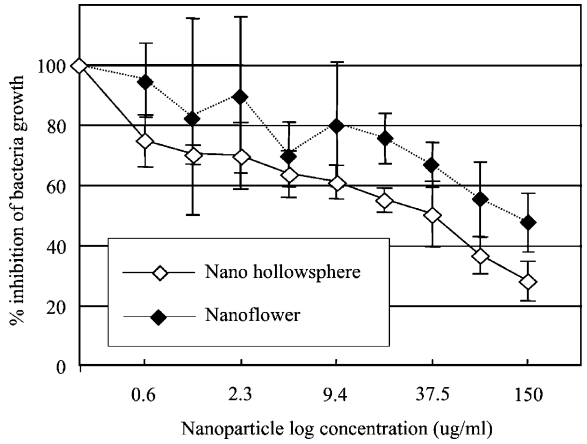

Figure 6. Bacteria growth inhibition for *Staphylococcus aureus* as referenced to the untreated control revealed dose-dependent antimicrobial activity of both hollow nanospheres (Au_3Cu_1) and nanoflowers ($Cu_2(OH)_3Cl$).

was also performed under a O_2 atmosphere, where no flowerlike structures were detected, but the wormlike morphology, which remained as a $Cu_2(OH)_3Cl$ structure, was observed (see Supporting Information). However, we did not want to exaggerate the role of the air moisture in the formation of nanoflowers since a certain amount of dissolved oxygen in the air may also contribute to the production of OH^- and thereafter $Cu_2(OH)_3Cl$.

Finally, we have shown the results for the formation of nanoflowers for the reaction period of 3 h. Extension of the reaction, for example to 12 h, would result in production of significant $Cu_2(OH)_3Cl$ crystals, and some of them may have interlaced together (see Supporting Information).

Nanoparticles with antimicrobial activity have been reported and are emerging as a new class of synthetic antibiotics and anti-microorganism surface treatment strategy. The introduction of these bactericidal nanoparticles not only gives a promising future and new thoughts for the treatment of antibiotic resistant microorganisms but also opens broad potential applications to fulfill the increasing general demands for hygiene in daily life. Both silver and copper were well-known to present antibacteria effects.[23,24] Copper oxides have recently been reported to enhance antibacterial activity of fabrics.[24] We therefore examined the antimicrobial activity of the as-synthesized hollow nanospheres and nanoflowers to an important common human pathogen, the *Staphylococcus aureus*. As shown in Figure 6, antimicrobial activities of both nanomaterials were observed. However, the hollow nanospheres showed stronger antibacteria effect than the nanoflowers with the MIC_{50} of 39.6 and 127.2 μg/mL, respectively. These results encouraged further development for both nanoparticles in the future antimicrobial surface treatment applications for infectious pathogen. In fact, we have also investigated both flakelike and wormlike materials. Although the antimicrobial mechanisms remained to be resolved, these $Cu_2(OH)_3Cl$ exhibiting flowerlike, flakelike, and wormlike structures do exhibit different degrees of antimicrobial activity. We are currently studying the bioactivity of these Au_3Cu_1 and $Cu_2(OH)_3Cl$ nanomaterials.

Conclusion

In summary, a fast solid evacuation process was observed to form Au_3Cu_1 hollow nanostructures by reaction of Cu nanoparticles with $HAuCl_4$. Following the aging, the botallackite $Cu_2(OH)_3Cl$ nanoflowers were readily generated and were proposed from a hollow nanospheres-mediated mineralization process. Both hollow nanospheres and nanoflowers presented antibacteria activity toward a common human pathogen *Staphylococcus aureus*, which could be further applied for antibacteria surface treatment or new antiinfectious agents. In addition, it has been found that biomolecules could have played an important role in determining the structures and properties for copper minerals. Further studies which incorporate simple amino acids, such as glycine and histine, will be explored to unveil morphology and nanostructures in the formation of $Cu_2(OH)_3Cl$ biominerals.

Acknowledgment. Funding from the Center for Micro/Nano Technology Research, National Cheng Kung University, under projects from the Ministry of Education and the National Science Council of Taiwan, is gratefully acknowledged. We also thank Dr. You-Chen Liu and I-Hsiao Chen for their contribution in the micro-MIC assay.

Supporting Information Available: UV−vis, EDX, XRD, TEM, and SEM images of the prepared products under the different experimental conditions. This material is available free of charge via the Internet at http://pubs.acs.org.

References and Notes

(1) Lichtenegger, H. C.; Schöberl, T.; Bartl, M. H.; Waite, H.; Stucky, G. D. *Science* **2002**, *298*, 389.

(2) Zhu, C. L.; Chen, C. N. Hao, L. Y.; Hu, Y.; Chen, Z. Y. *J. Cryst. Growth* **2004**, *263*, 473.

(3) Li, Y. B.; Bando, Y.; Golberg, D. *Appl. Phys. Lett*. **2003**, *82*, 1962.

(4) Takahashi, N.; Niwa, A.; Sugiura, H.; Nakamura, T. *Chem. Commun. (Cambridge)* **2003**, 318.

(5) Chen, A.; Peng X.; Koczkur, K.; Miller, B. *Chem. Commun. (Cambridge)* **2004**, 1964.
(6) Li, X. L.; Ge, J. P.; Li, Y. D. *Chem. Eur. J.* **2004**, *10*, 6163.
(7) Li, S.; Zhang, H.; Xu, J.; Yang, D. *Mater. Lett.* **2005**, *59*, 420.
(8) Zhang, H.; Yang, D.; Ma, X.; Ji, Y.; Xu, J.; Que, D. *Nanotechnology* **2004**, *15*, 622.
(9) Gorai, S.; Ganguli, D.; Chaudhuri, S. *Mater. Lett.* **2005**, *59*, 826.
(10) Zhang, Z.; Shao, X.; Yu, H.; Wang, Y.; Han, M. *Chem. Mater.* **2005**, *17*, 332.
(11) Liu, S.; Yu, J.; Cheng, B.; Zhang, Q. *Chem. Lett.* **2005**, *34*, 564.
(12) Zhu, Y.; Yang, Q.; Zheng, H.; Yu, W.; Qian, Y. *Mater. Chem. Phys.* **2005**, *91*, 293.
(13) Helander, I. M.; Nurmiaho-Lassila, E. L.; Ahvenainen, R.; Rhoades, J.; Roller, S. *Int. J. Food Microbiol.* **2001**, *71*, 235.
(14) Kubanek, J.; Jensen, P. R.; Keifer, P. A.; Sullards, M. C.; Collins, D. O.; Fenical, W. *Proc. Natl. Acad. Sci. U.S.A.* **2003**, *100*, 6916.
(15) (a) Yeh, M. S.; Yang, Y. S.; Lee, Y. P.; Lee, H. F.; Yeh, Y. H.; Yeh, C. S. *J. Phys. Chem. B* **1999**, *103*, 6851. (b) Chen, T. Y.; Chen, S. F.; Sheu, H. S.; Yeh, C. S. *J. Phys. Chem. B* **2002**, *106*, 9717.
(16) (a) Sun, Y.; Mayers, B.; Xia, Y. *Nano. Lett.* **2002**, *2*, 481. (b) Sum, Y.; Xia, Y. *Nano. Lett.* **2003**, *3*, 1569. (c) Sun, Y.; Mayers, B.; Xia, Y. *Adv. Mater.* **2003**, *15*, 641.
(17) Smigelskas, A. D.; Kirkendall, E. O. *Trans. Am. Inst. Min., Metall. Pet. Eng.* **1947**, *171*, 130.
(18) Yin, Y.; Rioux, R. M.; Erdonmez, C. K.; Hughes, S.; Somorjai, G. A. Alivisatos, A. P. *Science* **2004**, *304*, 711.
(19) Gale, W. F.; Totemeier T. C. *Smithells Metals Reference Book*, 8th ed.; Elsevier: Oxford, U.K., 2004.
(20) Wang, Y.; Cai, L.; Xia, Y. *Adv. Mater.* **2005**, *17*, 473.
(21) Hawthorne, F. C. *Mineral. Mag.* **1985**, *49*, 87.
(22) In case a, once Cu nanoparticles were prepared by laser ablation of CuO powder in 2-propanol, the PVP polymer was added into Cu colloidal solution after removal of residual CuO powder. Following an incubation of 5 min, the excess PVP was centrifuged away. The PVP coating the Cu nanoparticles was then dispersed in 2-propanol, then $HAuCl_4$ was introduced, and the aforementioned procedure was followed to produce hollow nanospheres and nanoflowers. In case b, hollow nanoparticles were collected using centrifugation to separate from the supernatant (referred as 1) by following the reaction of Cu colloids with $HAuCl_4$. The hollow particles obtained were then redispersed into a mixture of 2-propanl and PVP to form Cu-based nanocage@PVP particles. Subsequently, the PVP-coated hollow nanospheres were collected from centrifugation. The resulting nanocage@PVP particles were added into original supernatant (1), which consisted of the same solution environment as the formation of nanoflowers.
(23) Baker, C.; Pradhan, A.; Pakstis, L.; Pochan, D. J.; Shah, S. I. *J. Nanosci. Nanotechnol.* **2005**, *5*, 244.
(24) Neel, E. A.; Ahmed, I.; Pratten, J.; Nazhat, S. N.; Knowles, J. C. *Biomaterials* **2005**, *26*, 2247.